Optimization of titanium and titanium alloy surface properties by ultra-short laser processing for improved antibacterial characteristics

D M Aceti[1,5], A Daskalova[1], L Angelova[1], E Filipov[1], L Sotelo[2,3], A Andreeva[4], A Trifonov[4] and I Buchvarov[4]

[1]Institute of Electronics, Bulgarian Academy of Sciences, 72 Tsarigradsko Chaussee, 1784, Sofia, Bulgaria
[2]Friedrich-Alexander-Universität Erlangen-Nürnberg, 91058 Erlangen, Germany
[3]Innovation-Institut für Nanotechnologie und korrelative Mikroskopie gGmbH, 91301 Forchheim, Germany
[4]Faculty of Physics, St. Kl. Ohridski University of Sofia, 5 J. Bourchier Blvd. 1164 Sofia, Bulgaria

E-mail: acetidm@gmail.com

Abstract. The aim of the current study is to improve in a one step process the properties of Ti and Ti alloy surfaces by enhancing their bioactivity in order to provide better conditions for microbial rejection. We propose to alter the biomaterial characteristics by a method alternative to the chemical ones, namely, non-contact processing of the surface by ultra-short laser pulses. The laser-induced modification results in a surface with different topographic features and an increased presence of oxides. We performed hierarchical laser patterning of the surface inducing the formation of areas covered by nanostructures, or laser-induced periodic surface structures (LIPSS), alternating with areas covered by micropillars in their turn surmounted by LIPSS. The increased roughness achieved due to the presence of micropillars, together with a marked presence of oxides, has been proven by several studies to enhance the biocompatibility of the material by improving the surface wettability and, furthermore, promoting the cells adhesion and osseointegration, while reducing the adhesion of pathogens.
The laser processed surface, consisting of a pattern of parallel lines, showed improved and anisotropic wettability. The water contact angle value decreased by ~10° in a direction orthogonal to the lines of the pattern, and by ~40° in a parallel direction.

1. Introduction

The application of diverse types of biomaterials for the creation of prosthetic implants needs to fulfil several requirements: mechanical and biological compatibility with the host tissues and resistance to wear and corrosion in biological environments. Titanium-based materials meet all the requirements to be an optimal candidate as an orthopedic implant material and have been proved to be superior compared to other metallic materials [1]. These materials are among the most widely used ones for bone prosthetic implants owing to their high strength and toughness, although their main advantage resides in the lightweight and in the lower Young modulus, compared to other metals used for bone implants as cobalt-

[5] To whom any correspondence should be addressed.

chrome alloys, stainless steel, or tantalum. The Young modulus is closer to the bone elastic modulus so that the stress shielding effect is less likely to occur. Moreover, titanium has been proven to be a bio-inert and corrosion resistant material. Under biological condition, it undergoes passivation by forming a stable layer (~10 nm) of TiO_2.

The surface morphology and topography of a material play a key role in its behavior in a biological environment in terms of interaction with cells and bacteria. Critical requirements are promoting cell proliferation [2] and differentiation [3] while avoiding bacteria adhesion [4] and biofilm formation [5].

The approach proposed by us uses Ti:sapphire laser processing to obtain a pattern consisting of a combination of micro- and nanostructures on the surface of commercially pure titanium (cp-Ti) and titanium grade 6 (Ti-6Al-4V). Laser processing appears to be preferable compared to other surface modification processes [6] (e.g. sand blasting, machining, plasma spray, etc.), as it does not require additional materials for coating and also eliminates the use of chemicals (e.g., acid etching) to form surface features. In addition, the use of ultra-short pulses makes the process more precise and cleaner, with less debris formation [7], while thermal damage is avoided [8].

The process of interaction between the laser pulses and the surface of Ti and Ti alloy leads to the formation of laser-induced periodic surface structures (LIPSS), a topographical structure that has been shown to eliminate bacterial adhesion [9], while positively affecting the cellular response in terms of alignment and differentiation [10]. The appearance of new surface features comes together with a modification of the surface chemistry leading to the formation of an amorphous layer of TiO_2 [11].

LIPSS has also been proven, under particular conditions, to reduce the coefficient of friction and wear of laser-treated surface materials [12]; the use of LIPSS with such an aim in a biological environment is yet to be well explored. Cunha et al. demonstrated [13] the effectiveness of LIPSS on Ti against proliferation of *Staphylococcus aureus*. The group of Lee et al. found that LIPSS induces cells alignment and increases their metabolism [14], while Gnilitskyi et al. observed improved cell adhesion and proliferation [15] due to the presence of LIPSS.

Although these structures are usually hydrophobic, the presence of microscale roughness, combined with LIPSS, provides an improved wettability [16] that facilitates the cells adhesion and differentiation [17], as well as the osseointegration due to the better interlocking between the material surface and the actual bone [18] compared to a smooth surface.

In this paper, we describe the formation of specific structures obtained by ultrashort laser processing and the corresponding physico-chemical properties. The ratio between the areas covered by the LIPSS only and by a combination of LIPSS and micro-pillars, as well as the pillars size, can be tuned by varying the processing parameters, namely, hatch distance and laser scan speed and power.

2. Material and methods

Commercially available pure titanium and titanium-6 aluminium-4 vanadium plates with sizes 20 mm×20 mm×2 mm and 10 mm×10 mm×1 mm were patterned employing a Ti:sapphire laser system generating pulses with duration $\tau < 130$ fs at the central wavelength of 800 nm and a repetition rate of 1 kHz with a peak power above 1 W.

The plates were positioned on a two-axis motorized translation stage controlled by LabVIEW software. The laser beam was focused using an achromatic bi-convex lens with a 1-cm diameter and 10-cm focal length. The beam diameter before the lens had a 7-mm diameter; a chopper was used to change the repetition rate to 500 Hz.

The patterned surfaces were obtained using a variety of sets of parameters – translation stage scan speed ranging from 0.125 mm/s to 16 mm/s, pulse energy fixed at 0.06 mJ and 0.12 mJ, distance between adjacent lines varying between 100 μm and 150 μm.

The material was processed in air at room temperature. The processed samples were ultrasonically cleaned in deionized water for 10 minutes; this procedure was repeated four times, and then the samples were rinsed in water and ethanol to eliminate any residual produced in the process.

The morphology obtained via femtosecond laser processing was observed and studied using atomic force microscopy (AFM) (MFP-3D Asylum Research, Oxford Instruments, UK), an optical profilometer

(Zeta-20, Zeta Instruments, USA), and scanning electron microscopy (SEM) (TM4000, Hitachi); the wettability tests were performed using a 10-µl drop of deionized water and the contact angle was evaluated by using ImageJ software for picture analysis. A Raman spectrometer (LabRAM HR Evolution, Horiva) was used to investigate the chemical composition of the surface before and after laser processing using a 10× objective and a 532-nm laser with a power of 1.68 W.

3. Results

The femtosecond laser treatment induced the formation of diverse topographic features depending on the process parameters. Similar results were observed for both cp-Ti and Ti-6Al-4V. The laser exposure induced the formation of LIPSS with a periodicity of ~600 nm in all cases.

At the scan speed of ~1 mm/s, grooves were formed on both materials in the center of the lines, corresponding to the area subject to a higher energy density; spikes were seen at lower values of the scan speed. Both topographies are surmounted by LIPSS, as shown in figure 1 (a, b). Higher scan speed values allow the formation of LIPSS only, see figure 1 (c, d).

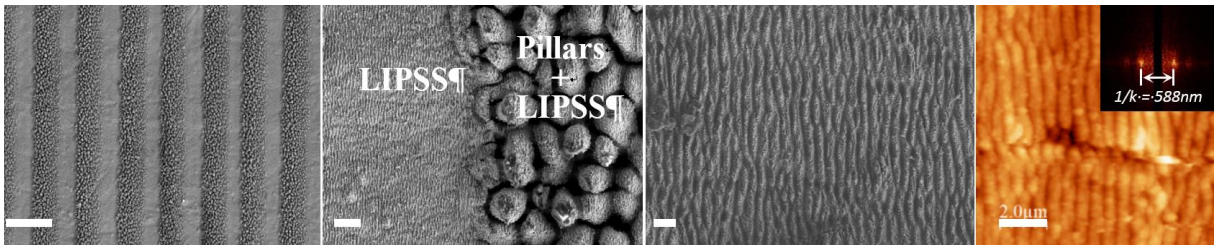

Figure 1. Surface morphology obtained by ultrashort laser processing, **a)** SEM micrograph, general appearance of the sample surface, laser power 60 mW, scan speed 0.25 mm/s, scale bar 100 µm; **b)** SEM micrograph, detail of the edge between the two kinds of morphology, laser power 60 mW, scan speed 0.25 mm/s, scale bar 5 µm; **c)** SEM micrograph of LIPSS only morphology, laser power 3 mW, scan speed 4 mm/s, scale bar 1 µm **d)** AFM topographic image of LIPSS, laser power 60 mW, scan speed 4 mm/s, the inset shows the 2D-FFT image highlighting the LIPSS period, scale bar 5 µm.

Using a laser power of 60 mW, scan speeds of 0.25 mm/s and 0.125 mm/s, and 100-µm distance between lines for cp-Ti and 150 µm for Ti-6Al-4V, half of the obtained surfaces is covered by LIPSS only, and half, by micropillars surmounted alternately by LIPSS. This composite morphology affects the properties of the surface. The first effect, due to the striped pattern, is the anisotropy in the wetting behavior in accordance with the direction of the laser-modeled lines. Generally, the drop spreads on the surface more easily in the direction parallel to the created lines, and less so along the perpendicular one. In the case of only LIPSS covering the surface, the hydrophobicity was improved; in contrast, the presence of micron-sized features improved the wettability of the surface. The water contact angle value is measured by observing the sample both along and across the laser-induced pattern lines; its value decreased by ~25° and ~10° respectively.

As seen in Figure 2, a higher pulse energy value is required to obtain a dense and homogeneous presence of pillars, while varying the scan speed affects the size of these structures. The longer exposure allows the pillars to become larger and eventually merge.

The Raman signal for the untreated material is of low intensity (see Figure 3), as expected for Raman scattering of metals; the presence of oxides becomes more evident while increasing the degree of modification of the surface. The absence of well-defined peaks is attributed to the formation of amorphous TiO_2; however, the presence of other kind of oxides, such as Ti_2O_3, cannot be excluded.

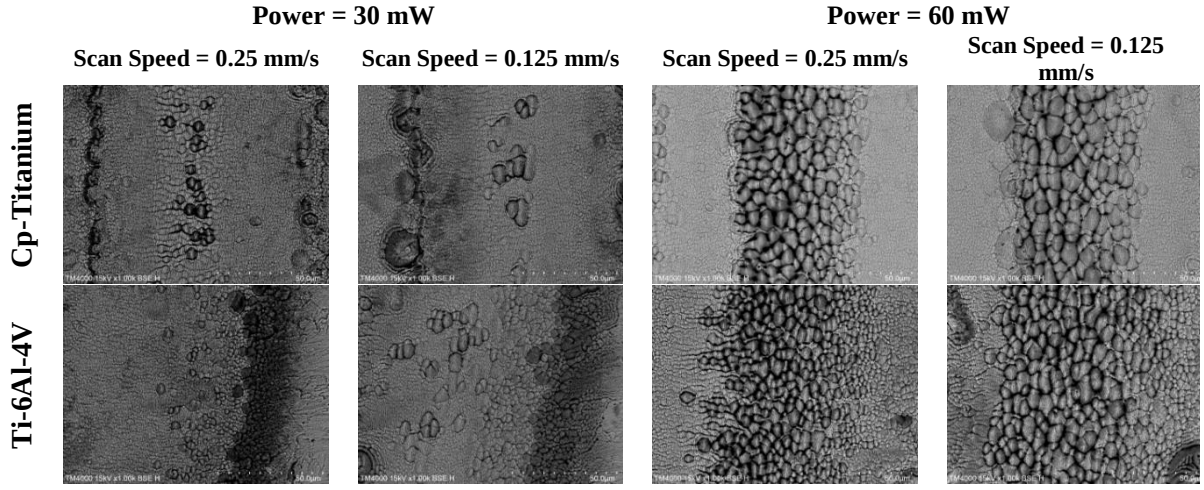

Figure 2. SEM micrographs of composite morphology obtained via fs laser processing on cp-Titanium and on Ti-6Al-4V with different process parameters. Scale bars are 50 μm.

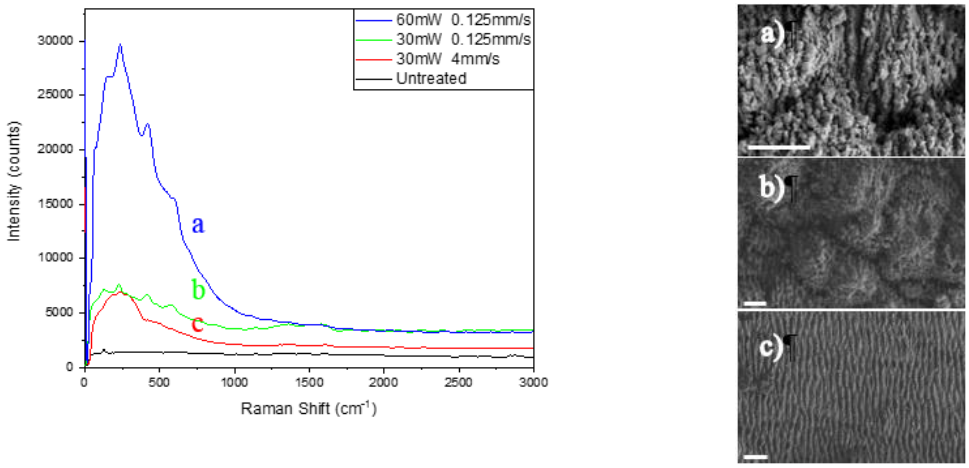

Figure 3. Raman spectra and the corresponding SEM micrographs of three different kinds of morphology. a) micropillars surmounted by LIPPS (blue line); b) incomplete formation of pillars covered by LIPSS (green line); surface covered by LIPPS only (red line). Scale bars are 2 μm.

4. Conclusions

Our study demonstrated that the ultrashort laser processing of a Ti surface results in a hierarchical morphology consisting of alternation of LIPSS only and of micropillars surmounted by LIPSS; at the same time, the formation of oxides increases, thus making the surface more hydrophilic. All these features are known to improve the biocompatibility and disadvantage the proliferation of bacteria.

The laser induced surface structuring provides a potentially favorable environment for the cells proliferation, while disfavoring the bacterial colonization. The hierarchical morphology can positively affect the cells adhesion and simultaneously lead to repelling or trapping of bacteria and preventing the formation of a biofilm. Our findings suggest that this approach can be widely applied to surface treatment of prosthetic materials, since no extreme conditions (e.g. vacuum) or additional chemicals (e.g. acids) are required and the process can be tailored according to specific needs.

Acknowledgments

This research has received funding from the European Union's H2020 research and innovation program under the Marie Sklodowska-Curie Grant Agreement No. 861138. The authors would like to

acknowledge the Bulgarian National Science Fund (NSF) under grant number No. KP-06-H48/6 (2020–2023) and project H2020 FET Open METAFAST Grant Agreement No. 899673.

References

[1] Geetha M, Singh A K, Asokamani R and Gogia A K 2009 *Progress in materials science* **54** (3) 397–425
[2] Ponsonnet L, Reybier K, Jaffrezic N, Comte V, Lagneau C, Lissac M and Martelet C 2003 *Materials Science and Engineering:* C **23** (4) 551–560
[3] Raines A L, Olivares-Navarrete R, Wieland M, Cochran D L, Schwartz Z and Boyan B D 2010 *Biomaterials* **31** (18) 4909–4917
[4] Cheng Y, Feng G and Moraru C I 2019 *Frontiers in microbiology* **10** 191
[5] Jaggessar A, Shahali H, Mathew A and Yarlagadda P K D V 2017 *Journal of nanobiotechnology* **15** (1) 1–20
[6] Gaggl A, Schultes G, Müller W D and Kärcher H 2000 *Biomaterials* **21** (10) 1067–1073
[7] Chichkov B N, Momma C, Nolte S, von Alvensleben F and Tünnermann A 1996 *Applied physics* A **63** (2) 109–115
[8] Phillips K C, Gandhi H H, Mazur E and Sundaram S K 2015 *Advances in Optics and Photonics* **7** (4) 684–712
[9] Lutey A H A, Gemini L, Romoli L, Lazzini G, Fuso F, Faucon M and Kling R 2018 *Scientific reports* **8** (1) 1–10
[10] Dumas V *et al.* 2015 *Biomedical Materials* **10** (5) 055002
[11] Landis E C, Phillips K C, Mazur E and Friend C M 2012 *Journal of Applied Physics* **112** (6) 063108
[12] Bonse J, Koter R, Hartelt M, Spaltmann D, Pentzien S, Höhm S, Rosenfeld A and Krüger J 2014 *Applied physics* A **117** (1) 103–110
[13] Cunha, Alexandre, Elie A-M, Plawinski L, Serro A P, Botelho do Rego A M, Almeida A, Urdaci M C, Durrieu M-C and Vilar R 2016 *Applied Surface Science* **360** 485–493
[14] Lee B E J, Exir H, Weck A and Grandfield K 2018 *Applied Surface Science* **441** 1034–1042
[15] Gnilitskyi I, Pogorielov M, Viter R, Ferraria A M, Carapeto A P, Oleshko O, Orazi L and Mishchenko O 2019 *Nanomedicine: Nanotechnology, Biology and Medicine* **21** 102036
[16] Klos A, Sedao X, Itina T E, Helfenstein-Didier C, Donnet C, Peyroche S, Vico L, Guignandon A and Dumas V 2020 *Nanomaterials* **10** (5) 864
[17] Pfleging W, Kumari R, Besser H, Scharnweber T and Majumdar J D 2015 *Applied Surface Science* **355** 104–111
[18] Shah F A, Simonsson H, Palmquist A and Thomsen P 2016 *PloS one* **11** (6) e0157504